

DEVELOPMENT OF A FINITE DYNAMIC ELEMENT FOR FREE VIBRATION ANALYSIS OF TWO-DIMENSIONAL STRUCTURES*

K. K. GUPTA†

Jet Propulsion Laboratory, California Institute of Technology, Pasadena, California, U.S.A.

SUMMARY

The paper develops an efficient free-vibration analysis procedure of two-dimensional structures. This is achieved by employing a discretization technique based on a recently developed concept of finite dynamic elements, involving higher order dynamic correction terms in the associated stiffness and inertia matrices.

A plane rectangular dynamic element is developed in detail. Numerical solution results of free-vibration analysis presented herein clearly indicate that these dynamic elements combined with a suitable quadratic matrix eigenproblem solution technique effect a most economical and efficient solution for such an analysis when compared with the usual finite element method.

INTRODUCTION

Numerical analysis of free-vibration problems of structures essentially consists of two distinct yet related procedures. First, the continuum is suitably discretized by the finite element method, yielding sets of algebraic simultaneous equations that define the associated eigenvalue problem. For many complex practical structures, the number of equations tends to become large, thereby rendering the solution rather uneconomical. As such, there appears to be a definite need for the development of special structural elements that yield a desired solution accuracy with lesser numbers of elements and, hence, degrees-of-freedom. Secondly, such a discretization of a continuum yields highly banded stiffness and inertia matrices when it would be most desirable to develop suitable eigenproblem solution techniques that fully exploit the associated matrix sparsity. This article is concerned with both of these aspects of the analysis. Thus, the development of a new rectangular element involving frequency-dependent stiffness and inertia matrices and pertaining to two-dimensional structures is given in detail. This is followed by a description of some efficient quadratic matrix eigenproblem solution techniques. Numerical results are also presented that strongly indicate that the newly developed element requires a much coarser mesh for a specified solution accuracy when compared with the usual finite element discretization. Furthermore, the eigenproblem solution techniques also prove to be most efficient in the solution of sparse banded matrices. Since the total free vibration solution time is dependent on the order and sparsity of such matrices, the present procedure results in significant solution economy.

* This paper presents the results of one phase of research carried out at the Jet Propulsion Laboratory, California Institute of Technology, for the Air Force Office of Scientific Research (AFOSR).

† Member of the Technical Staff, Structures and Materials Section.

The fundamental relationship in the finite element method that describes the continuous displacement field vector within an element in terms of its nodal displacements, is given by

$$\mathbf{u} = \mathbf{a}\mathbf{U} \quad (1)$$

which is only valid for static loading. For dynamic loading, \mathbf{u} is, in general, a function of the entire time history of the nodal displacements. On the other hand, for harmonic motions such as free vibrations, \mathbf{u} is unique in the sense that it is a function of the instantaneous nodal displacements. However, in such a case, \mathbf{a} is a function of the natural frequencies, thereby resulting in frequency-dependent stiffness and inertia matrices; the extraction of eigenvalues and vectors from such matrices is very uneconomical and almost prohibitive, since they are not known *a priori*. To circumvent such a situation the matrix \mathbf{a} is expressed in ascending powers of the natural frequency

$$\mathbf{a} = \mathbf{a}_0 + \omega \mathbf{a}_1 + \omega^2 \mathbf{a}_2 + \dots \quad (2)$$

resulting in the following expressions for the stiffness and inertia matrices¹

$$\mathbf{K} = \mathbf{K}_0 + \omega^4 \mathbf{K}_4 + \dots \quad (3)$$

$$\mathbf{M} = \mathbf{M}_0 + \omega^2 \mathbf{M}_2 + \dots \quad (4)$$

The associated equation of motion for free vibration has the following form:

$$[\mathbf{K}_0 - \omega^2 \mathbf{M}_0 - \omega^4 (\mathbf{M}_2 - \mathbf{K}_4) - \dots] \mathbf{q} = \mathbf{0} \quad (5)$$

in which \mathbf{K}_0 and \mathbf{M}_0 are the static stiffness and inertia matrices pertaining to the usual finite element method, the matrices \mathbf{M}_2 and \mathbf{K}_4 constitute the dynamic correction terms and \mathbf{q} is the amplitude of \mathbf{U} . In the usual finite element free-vibration analysis, only the first two terms in equation (5) are retained for the solution. However, inclusion of the third term in equation (5) is known to effect substantial improvements in root convergence for one-dimensional structures.^{1,2} Such dynamic correction matrices have been recently developed for the first time³ for a continuum, discretized by prestressed membrane elements, and the resulting improvement in the convergence pattern of the natural frequencies and vectors was found to be most significant in nature. Throughout this article the discretization process involving finite 'dynamic' elements employing higher order dynamic correction terms will be referred to as the dynamic element method (DEM), as opposed to the usual finite element method (FEM) involving static finite elements.

By retaining the first three terms in equation (5), the quadratic matrix eigenvalue problem is written in a general form

$$(\mathbf{A} - \lambda \mathbf{B} - \lambda^2 \mathbf{C}) \mathbf{q} = \mathbf{0} \quad (6)$$

with $\lambda = \omega^2$ and when it is noted that the matrices \mathbf{A} , \mathbf{B} and \mathbf{C} are positive definite in nature, being of highly banded configurations for most practical structures. It would, thus, be highly desirable to also develop efficient eigenvalue routines that fully exploit such matrix sparsity, thereby enabling economical solution of large, complex practical structures. Solution of equation (6) has been achieved earlier¹ by first rearranging the same as follows:

$$(\mathbf{G} - \lambda \mathbf{I}_{2n}) \hat{\mathbf{y}} = \mathbf{0} \quad (7)$$

in which

$$\mathbf{G} = \begin{bmatrix} \mathbf{0} & \mathbf{I}_n \\ \mathbf{C}^{-1} \mathbf{A} & -\mathbf{C}^{-1} \mathbf{B} \end{bmatrix}, \quad \hat{\mathbf{y}} = \begin{bmatrix} \mathbf{q} \\ \dot{\mathbf{q}} \end{bmatrix}, \quad \dot{\mathbf{q}} = \lambda \mathbf{q} \quad (7a)$$

n being the order of the associated matrices and \mathbf{I} the identity matrix. The eigenvalue problem of equation (7) may be solved by such standard methods such as QR or Lanczos's. However, such a solution would prove to be rather uneconomical since the matrix \mathbf{G} is unsymmetric and of order $2n$, being also almost full in nature.

A number of quadratic matrix eigenvalue routines, however, have been recently developed that fully exploit the matrix sparsity of the individual matrices of equation (5). This has been achieved by employing various Sturm sequence, inverse iteration, and simultaneous iteration techniques.²⁻⁴ Development of such techniques goes hand-in-hand with the generation of new finite dynamic elements, since the two processes, when combined, produce a highly efficient free vibration analysis capability.

The following section presents the complete details of the development of a plane rectangular dynamic element pertaining to a two-dimensional structural continuum. A summary of the various quadratic matrix eigenproblem solution techniques is also provided in some detail. Numerical examples are presented next which provide a comparison between the usual finite element and the dynamic element analysis results. This is followed by general discussions on the relative efficiencies of the two analyses procedures which confirm that adoption of the present solution technique results in most significant economy in the solution of structural free vibration problems.

DEVELOPMENT OF THE FINITE DYNAMIC ELEMENT AND ASSOCIATED NUMERICAL SCHEMES

This section firstly describes the details of a plane rectangular finite dynamic element developed for the solution of two-dimensional structures such as plane-stress and plane-strain problems. The later part of the section provides a summary of efficient quadratic matrix eigenproblem solution schemes.

A plane rectangular dynamic element

Figure 1 depicts a plane rectangular element; the differential equations of motion of such an element undergoing free vibration may be expressed as

$$\frac{\partial^2 u_x}{\partial x^2} + \frac{\partial^2 u_x}{\partial y^2} + \frac{1}{(1-2\mu)} \frac{\partial}{\partial x} \left(\frac{\partial u_x}{\partial x} + \frac{\partial u_y}{\partial y} \right) = 2(1+\mu) \frac{\rho}{E} \frac{\partial^2 u_x}{\partial t^2} \quad (8)$$

$$\frac{\partial^2 u_y}{\partial x^2} + \frac{\partial^2 u_y}{\partial y^2} + \frac{1}{(1-2\mu)} \frac{\partial}{\partial y} \left(\frac{\partial u_x}{\partial x} + \frac{\partial u_y}{\partial y} \right) = 2(1+\mu) \frac{\rho}{E} \frac{\partial^2 u_y}{\partial t^2} \quad (9)$$

in which u_x , u_y are the in-plane deformations, μ , ρ and E being Poisson's ratio, the mass of the element per unit area and Young's modulus, respectively. The solution of equations (8) and (9) may be assumed in the following infinite series form

$$u_x = \sum_{r=0}^{\infty} \omega^r \mathbf{a}_{rx} \mathbf{q} e^{i\omega t} \quad (10)$$

$$u_y = \sum_{r=0}^{\infty} \omega^r \mathbf{a}_{ry} \mathbf{q} e^{i\omega t} \quad (11)$$

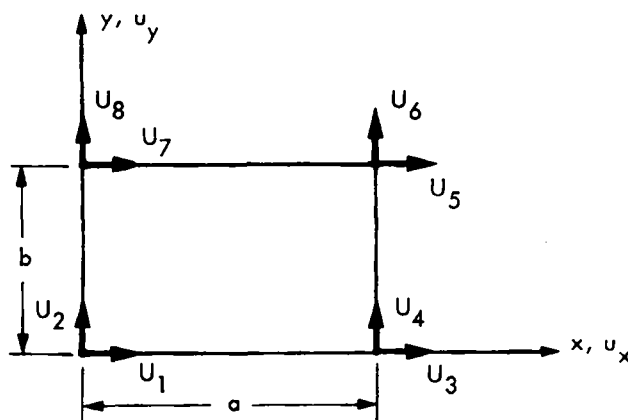


Figure 1. Rectangular plane element

which when substituted in equations (8) and (9) yields the following equations of motion:

$$\sum_{r=0}^{\infty} \omega^r \frac{\partial^2 \mathbf{a}_{rx}}{\partial x^2} \mathbf{q} e^{i\omega t} + \sum_{r=0}^{\infty} \frac{\partial^2 \mathbf{a}_{rx}}{\partial y^2} \mathbf{q} e^{i\omega t} + \frac{1}{(1-2\mu)} \sum_{r=0}^{\infty} \omega^r \frac{\partial^2 \mathbf{a}_{rx}}{\partial x^2} \mathbf{q} e^{i\omega t} + \frac{1}{(1-2\mu)} \sum_{r=0}^{\infty} \omega^r \frac{\partial^2 \mathbf{a}_{ry}}{\partial x \partial y} \mathbf{q} e^{i\omega t} = -2(1+\mu) \frac{\rho}{E} \omega^2 \sum_{r=0}^{\infty} \omega^r \mathbf{a}_{rx} \mathbf{q} e^{i\omega t} \quad (12)$$

$$\sum_{r=0}^{\infty} \omega^r \frac{\partial^2 \mathbf{a}_{ry}}{\partial x^2} \mathbf{q} e^{i\omega t} + \sum_{r=0}^{\infty} \omega^r \frac{\partial^2 \mathbf{a}_{ry}}{\partial y^2} \mathbf{q} e^{i\omega t} + \frac{1}{(1-2\mu)} \sum_{r=0}^{\infty} \frac{\partial^2 \mathbf{a}_{rx}}{\partial x \partial y} \mathbf{q} e^{i\omega t} + \frac{1}{(1-2\mu)} \sum_{r=0}^{\infty} \omega^r \frac{\partial^2 \mathbf{a}_{ry}}{\partial y^2} \mathbf{q} e^{i\omega t} = -2(1+\mu) \frac{\rho}{E} \omega^2 \sum_{r=0}^{\infty} \omega^r \mathbf{a}_{ry} \mathbf{q} e^{i\omega t} \quad (13)$$

In the subsequent analysis, only the first three terms of equations (10) and (11) are retained. Equating the coefficients of the same powers of ω , equations (12) and (13) yield the following differential equations

$$\frac{\partial^2 \mathbf{a}_{0x}}{\partial x^2} + \frac{\partial^2 \mathbf{a}_{0x}}{\partial y^2} + \frac{1}{(1-2\mu)} \left(\frac{\partial^2 \mathbf{a}_{0x}}{\partial x^2} + \frac{\partial^2 \mathbf{a}_{0y}}{\partial x \partial y} \right) = 0 \quad (14)$$

$$\frac{\partial^2 \mathbf{a}_{1x}}{\partial x^2} + \frac{\partial^2 \mathbf{a}_{1x}}{\partial y^2} + \frac{1}{(1-2\mu)} \left(\frac{\partial^2 \mathbf{a}_{1x}}{\partial x^2} + \frac{\partial^2 \mathbf{a}_{1y}}{\partial x \partial y} \right) = 0 \quad (15)$$

$$\alpha_1 \frac{\partial^2 \mathbf{a}_{2x}}{\partial x^2} + \frac{\partial^2 \mathbf{a}_{2x}}{\partial y^2} + \alpha_2 \frac{\partial^2 \mathbf{a}_{2y}}{\partial x \partial y} = -\beta \mathbf{a}_{0x} \quad (16)$$

and

$$\frac{\partial^2 \mathbf{a}_{0y}}{\partial x^2} + \frac{\partial^2 \mathbf{a}_{0y}}{\partial y^2} + \frac{1}{(1-2\mu)} \left(\frac{\partial^2 \mathbf{a}_{0y}}{\partial y^2} + \frac{\partial^2 \mathbf{a}_{0x}}{\partial x \partial y} \right) = 0 \quad (17)$$

$$\frac{\partial^2 \mathbf{a}_{1y}}{\partial x^2} + \frac{\partial^2 \mathbf{a}_{1y}}{\partial y^2} + \frac{1}{(1-2\mu)} \left(\frac{\partial^2 \mathbf{a}_{1y}}{\partial y^2} + \frac{\partial^2 \mathbf{a}_{1x}}{\partial x \partial y} \right) = 0 \quad (18)$$

$$\alpha_1 \frac{\partial^2 \mathbf{a}_{2y}}{\partial y^2} + \frac{\partial^2 \mathbf{a}_{2y}}{\partial x^2} + \alpha_2 \frac{\partial^2 \mathbf{a}_{2x}}{\partial x \partial y} = -\beta \mathbf{a}_{0y} \quad (19)$$

with

$$\alpha_1 = \frac{2(1-\mu)}{(1-2\mu)}, \quad \alpha_2 = \frac{1}{(1-2\mu)} \quad \text{and} \quad \beta = 2(1+\mu) \frac{\rho}{E}$$

Equations, as above, are solved by using \mathbf{a}_{0x} and \mathbf{a}_{0y} to satisfy the boundary conditions that

$$u_x = U_1, u_y = U_2 \quad \text{at } x = 0, y = 0 \quad u_x = U_3, u_y = U_4 \quad \text{at } x = a, y = 0$$

$$u_x = U_5, u_y = U_6 \quad \text{at } x = a, y = b \quad \text{and} \quad u_x = U_7, u_y = U_8 \quad \text{at } x = 0, y = b$$

while postulating that \mathbf{a}_{1x} , \mathbf{a}_{1y} and \mathbf{a}_{2x} , \mathbf{a}_{2y} must all vanish at the boundaries.^{1,3}

The solutions for the two homogeneous equations (14) and (17) are taken in the following form,¹ based on a linear-edge-displacement assumption

$$\mathbf{a}_{0x} \mathbf{U} = C_1 + C_2 x + C_3 y + C_4 xy \quad (20)$$

$$\mathbf{a}_{0y} \mathbf{U} = C_5 + C_6 x + C_7 y + C_8 xy \quad (21)$$

where the coefficients C_1 – C_8 are evaluated by satisfying the boundary conditions, appropriately. Similar series solutions are adopted for equations (15) and (18), whereas the solutions for equations (16) and (19) are assumed as follows:

$$\begin{aligned} \mathbf{a}_{2x} \mathbf{U} = A_1 + A_2 x + A_3 y + A_4 xy - \beta \left[\frac{C_1}{4} \frac{x^2}{\alpha_1} + \frac{C_1}{4} y^2 + \frac{C_2}{12} \frac{x^3}{\alpha_1} + \frac{C_2}{4} xy^2 \right. \\ \left. + \frac{C_3}{4} \frac{x^2 y}{\alpha_1} + \frac{C_3}{12} y^3 + \frac{C_4}{12} \frac{x^3 y}{\alpha_1} + \frac{C_4}{12} xy^3 \right] \quad (22) \end{aligned}$$

$$\begin{aligned} \mathbf{a}_{2y} \mathbf{U} = A_5 + A_6 x + A_7 y + A_8 xy - \beta \left[\frac{C_5}{4} \frac{y^2}{\alpha_1} + \frac{C_5}{4} x^2 + \frac{C_6}{12} x^3 + \frac{C_6}{4} \frac{xy^2}{\alpha_1} \right. \\ \left. + \frac{C_7}{4} x^2 y + \frac{C_7}{12} \frac{y^3}{\alpha_1} + \frac{C_8}{12} x^3 y + \frac{C_8}{12} \frac{xy^3}{\alpha_1} \right] \quad (23) \end{aligned}$$

in which the coefficients A_1 – A_8 pertaining to the complementary functions are obtained by satisfying the appropriate boundary conditions, when it may be noted that the coefficients C_1 – C_8 are computed earlier from equations (20) and (21). The final solutions are obtained after some algebraic manipulations:

$$\mathbf{a}_{0x} = \mathbf{a}_{0y} = \left[\left(\frac{xy}{ab} - \frac{x}{a} - \frac{y}{b} + 1 \right) \left(\frac{x}{a} - \frac{xy}{ab} \right) \frac{xy}{ab} \left(\frac{y}{b} - \frac{xy}{ab} \right) \right] \quad (24)$$

$$\mathbf{a}_{1x} = \mathbf{a}_{1y} = 0$$

$$\mathbf{a}_{2x}^T = \beta \left[\begin{aligned} & \left(-\frac{xy^3}{12ab} + \frac{y^3}{12b} + \frac{xy^2}{4a} - \frac{y^2}{4} - \frac{x^3 y}{12\alpha_1 ab} + \frac{x^2 y}{4\alpha_1 b} - \frac{bxy}{6a} - \frac{axy}{6\alpha_1 b} \right. \\ & \qquad \qquad \qquad \left. + \frac{by}{6} + \frac{x^3}{12\alpha_1 a} - \frac{x^2}{4\alpha_1} + \frac{ax}{6\alpha_1} \right) \\ & \left(\frac{xy^3}{12ab} - \frac{xy^2}{4a} + \frac{x^3 y}{12\alpha_1 ab} + \frac{bxy}{6a} - \frac{axy}{12\alpha_1 b} - \frac{x^3}{12\alpha_1 a} + \frac{ax}{12\alpha_1} \right) \\ & \left(-\frac{xy^3}{12ab} - \frac{x^3 y}{12\alpha_1 ab} + \frac{bxy}{12a} + \frac{axy}{12\alpha_1 b} \right) \\ & \left(\frac{xy^3}{12ab} - \frac{y^3}{12b} + \frac{x^3 y}{12\alpha_1 ab} - \frac{x^2 y}{4\alpha_1 b} - \frac{bxy}{12a} + \frac{axy}{6\alpha_1 b} + \frac{by}{12} \right) \end{aligned} \right] \quad (25)$$

$$\mathbf{a}_{2y}^T = \beta \left[\begin{array}{l} \left(-\frac{xy^3}{12\alpha_1 ab} + \frac{y^3}{12\alpha_1 b} + \frac{xy^2}{4\alpha_1 a} - \frac{y^2}{4\alpha_1} - \frac{x^3 y}{12ab} + \frac{x^2 y}{4b} - \frac{bxy}{6\alpha_1 a} - \frac{axy}{6b} \right. \\ \left. + \frac{by}{6\alpha_1} + \frac{x^3}{12a} - \frac{x^2}{4} + \frac{ax}{6} \right) \\ \left(\frac{xy^3}{12\alpha_1 ab} - \frac{xy^2}{4\alpha_1 a} + \frac{x^3 y}{12ab} + \frac{bxy}{6\alpha_1 a} - \frac{axy}{12b} - \frac{x^3}{12a} + \frac{ax}{12} \right) \\ \left(-\frac{xy^3}{12\alpha_1 ab} - \frac{x^3 y}{12ab} + \frac{bxy}{12\alpha_1 a} + \frac{axy}{12b} \right) \\ \left(\frac{xy^3}{12\alpha_1 ab} - \frac{y^3}{12\alpha_1 b} + \frac{x^3 y}{12ab} - \frac{x^2 y}{4b} - \frac{bxy}{12\alpha_1 a} + \frac{axy}{6b} + \frac{by}{12\alpha_1} \right) \end{array} \right] \quad (26)$$

The vector \mathbf{a} is now defined as

$$\left. \begin{array}{l} \mathbf{a}_x = \mathbf{a}_{0x} + \omega^2 \mathbf{a}_{2x} \\ \mathbf{a}_y = \mathbf{a}_{0y} + \omega^2 \mathbf{a}_{2y} \end{array} \right\} \quad (27)$$

when it should be noted that the elements of each of the above vectors couple with the appropriate nodal degrees-of-freedom; furthermore, the expressions for \mathbf{a}_{0x} , \mathbf{a}_{0y} may also be obtained by direct use of Lagrange's interpolation formula. Strain-displacement relations are given by

$$\left. \begin{array}{l} \varepsilon_{xx} = \frac{\partial u_x}{\partial x} = \frac{\partial \mathbf{a}_{0x}}{\partial x} \mathbf{U} + \omega^2 \frac{\partial \mathbf{a}_{2x}}{\partial x} \mathbf{U} = (\mathbf{b}_{0xx} + \omega^2 \mathbf{b}_{2xx}) \mathbf{U} \\ \varepsilon_{yy} = \frac{\partial u_y}{\partial y} = \frac{\partial \mathbf{a}_{0y}}{\partial y} \mathbf{U} + \omega^2 \frac{\partial \mathbf{a}_{2y}}{\partial y} \mathbf{U} = (\mathbf{b}_{0yy} + \omega^2 \mathbf{b}_{2yy}) \mathbf{U} \\ \varepsilon_{xy} = \frac{\partial u_x}{\partial y} + \frac{\partial u_y}{\partial x} = \frac{\partial \mathbf{a}_{0x}}{\partial y} \mathbf{U} + \frac{\partial \mathbf{a}_{0y}}{\partial x} \mathbf{U} + \omega^2 \left(\frac{\partial \mathbf{a}_{2x}}{\partial y} \mathbf{U} + \frac{\partial \mathbf{a}_{2y}}{\partial x} \mathbf{U} \right) \\ = (\mathbf{b}_{0xy} + \omega^2 \mathbf{b}_{2xy}) \mathbf{U} \end{array} \right\} \quad (28)$$

or

$$\mathbf{e} = \mathbf{b} \mathbf{U} \quad (28a)$$

The strain-displacement matrices are appropriately combined to yield

$$\mathbf{b} = \mathbf{b}_0 + \omega^2 \mathbf{b}_2 \quad (29)$$

The foregoing relationships may next be conveniently employed to develop the stiffness and inertia matrices of the dynamic element. Thus the stiffness matrices are obtained from

$$\mathbf{k} = \int_v \mathbf{b}^T \boldsymbol{\chi} \mathbf{b} \, dV \quad (30)$$

where $\boldsymbol{\chi}$ is the standard stress-strain matrix for two-dimensional elasticity (Reference 1, p. 17); the individual element stiffness matrices corresponding to equation (3) are computed as below:

$$\mathbf{k}_0 = \int_v \mathbf{b}_0^T \boldsymbol{\chi} \mathbf{b}_0 \, dV \quad (31)$$

$$\mathbf{k}_4 = \int_v \mathbf{b}_2^T \boldsymbol{\chi} \mathbf{b}_2 \, dV \quad (32)$$

Similarly the element inertia matrices are obtained from

$$\mathbf{m}_{0x} = \rho \int_v \mathbf{a}_{0x}^T \mathbf{a}_{0x} dV \quad (33)$$

$$\mathbf{m}_{0y} = \rho \int_v \mathbf{a}_{0y}^T \mathbf{a}_{0y} dV \quad (34)$$

$$\mathbf{m}_{2x} = \rho \left(\int_v \mathbf{a}_{0x}^T \mathbf{a}_{2x} dV + \int_v \mathbf{a}_{2x}^T \mathbf{a}_{0x} dV \right) \quad (35)$$

$$\mathbf{m}_{2y} = \rho \left(\int_v \mathbf{a}_{0y}^T \mathbf{a}_{2y} dV + \int_v \mathbf{a}_{2y}^T \mathbf{a}_{0y} dV \right) \quad (36)$$

which are appropriately combined to yield the \mathbf{m}_0 and \mathbf{m}_2 matrices corresponding to equation (4), each being of dimension 8×8 .

From the nature and complexity of the various numerical processes including the integration schemes, as above, it is quite apparent that, for all practical purposes, it may not be possible to perform all such operations manually. The MIT symbolic and numerical manipulation programming system MACSYMA⁵ has thus been extensively utilized for the evaluation of \mathbf{a} , \mathbf{b} , \mathbf{k} and \mathbf{m} matrices and their various components as depicted by equations (20)–(36). The FORTRAN expressions for the element inertia and stiffness matrices are included in subroutine ELEMENT, which is presented in the Appendix, being directly printed out by MACSYMA, in which the element side lengths a , b are represented by A and B , respectively. Such matrices are combined by the usual process to yield the corresponding global matrices pertaining to the entire structure to form the quadratic matrix eigenvalue problem as represented by equations (5) and (6).

Solution of the quadratic matrix eigenproblem

The associated matrices \mathbf{A} , \mathbf{B} and \mathbf{C} of the eigenvalue problem of equation (6) are usually of highly banded configurations for most practical problems. An efficient quadratic matrix eigenproblem solution routine thus must exploit such matrix sparsity to enable efficient and economical solution of large complex practical problems. To implement such a solution scheme, equation (6) is first rearranged as below

$$\left(\begin{bmatrix} \mathbf{C} & \mathbf{0} \\ \mathbf{0} & \mathbf{A} \end{bmatrix} - \omega^2 \begin{bmatrix} \mathbf{0} & \mathbf{C} \\ \mathbf{C} & \mathbf{B} \end{bmatrix} \right) \begin{Bmatrix} \dot{\mathbf{q}} \\ \mathbf{q} \end{Bmatrix} = \mathbf{0} \quad (37)$$

which may also be written as

$$(\mathbf{E} - \omega^2 \mathbf{F}) \mathbf{y} = \mathbf{0} \quad (38)$$

where the matrices \mathbf{E} and \mathbf{F} are symmetric, \mathbf{E} being also positive-definite in nature. A Sturm sequence method² in conjunction with a bisection technique has earlier been adopted for the solution of equation (37), which exploits the associated matrix sparsity and also enables computation of a few desired roots without having to compute any other. Further improvement in the solution of the quadratic matrix problem was achieved by adopting a combined Sturm sequence and inverse iteration technique, the details of which are given in References 3 and 4, and only a brief summary of the same is given next.

Thus, the required roots are first isolated by the Sturm sequence method employing a bisection strategy. The middle point of the bound of each such isolated root is next used as the

starting root iteration value of the inverse iteration procedure that effects simultaneous determination of the roots and their corresponding vectors. Thus, the procedure involves the following iteration scheme

$$(\mathbf{E} - (\omega'_m)^2 \mathbf{F}) \mathbf{y}'_{i+1} = x_{i+1} \mathbf{F} \mathbf{y}'_i \quad (39)$$

at a typical $(i + 1)$ th iteration for the n th root which is effected by first reducing the lower half

$$[\mathbf{A} - (\omega'_m)^2 \mathbf{B} - (\omega'_m)^4 \mathbf{C}] \mathbf{q}'_{i+1} = x_{i+1} [\mathbf{C} \mathbf{q}'_i + \mathbf{B} \mathbf{q}'_i + (\omega'_m)^2 \mathbf{C} \mathbf{q}'_i] \quad (40)$$

which is followed by the simple solution of the equation in the upper half

$$\mathbf{C} \mathbf{q}'_{i+1} - (\omega'_m)^2 \mathbf{C} \mathbf{q}'_{i+1} = x_{i+1} \mathbf{C} \mathbf{q}'_i \quad (41)$$

where x_{i+1} is a normalizing factor, $\omega'_m = (\omega'_u + \omega'_l)/2$, ω'_u , ω'_l being, respectively, the upper and lower bound of the root isolated in the earlier process. A new estimate of ω' is next obtained using the Rayleigh quotient, and the process is repeated until the desired convergence is achieved. The solution time for this procedure is proportional to $1.5 nm^2 (NR) (NT)$; n and $m + 1$ are the order and half bandwidth of \mathbf{A} , NR is the number of required roots, NT being the number of reductions of $\mathbf{A} - \omega^2 \mathbf{B} - \omega^4 \mathbf{C}$ averaging about three per root. For an in-core solution the average storage requirement amounts to $[(m + 1)(2m + 1) + n(2m + 1) + n(m + 1)]$ words, although for an out-of-core solution only $(m + 1)(2m + 1)$ words are the usual requirement. An alternative algorithm based on a simultaneous iteration technique⁶ has also been presented earlier⁴ that proves to be efficient when the first few roots are the usual requirement.

NUMERICAL RESULTS

A square cantilever plate (Figure 2), vibrating in its own plane, was chosen as an example to demonstrate the relative efficiency of the rectangular plane dynamic element developed in this paper, over the usual associated finite element. Numerical results were thus obtained employing both static and dynamic elements. Such results are computed in parametric form using the following basic data

$$\text{Poisson's ratio } (\mu) = 0.3$$

$$\text{Thickness } (t) = 1.0$$

$$\text{Side lengths } (l_x, l_y) = 10.0$$

The cantilever plate was discretized by an increasing number of elements and the natural frequencies and associated modes computed for a number of idealizations; such results are given in Table I, whereas Figure 2 also presents a few mode shapes. Except for the DEM analysis for ω_2 , convergence to the respective roots for all other cases, are found to be approached from above.

Figure 3 shows the pattern of root convergence for two typical roots, for varying mesh sizes, whereas Figure 4 shows the variation of error in frequencies as a function of the total computational effort expended in the solution of the free vibration problem. Since no exact analytical solution of the cantilever plate problem was found in the literature, an analysis was performed employing a rather fine mesh of dimension 20×20 . Such a result forms the basis for establishing the pattern of root convergence, as presented in this section.

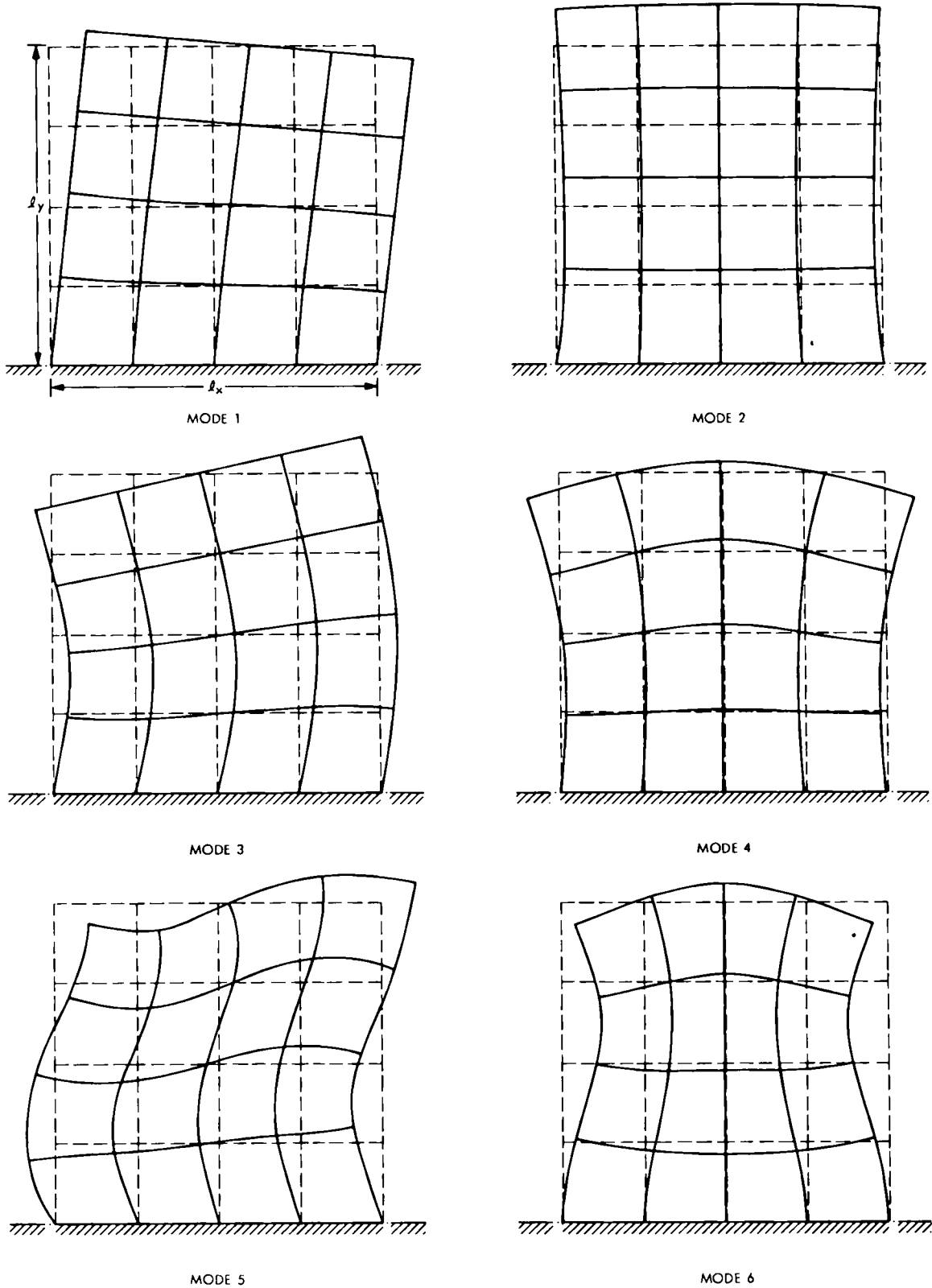


Figure 2. Mode shapes of a cantilever plate vibrating in its own plane

Table I. Natural frequencies of a square cantilever plate: (FEM results in upper rows, DEM results in lower rows)

Mesh size	Eigenvalue parameters $\hat{\omega} = \omega/\sqrt{(E/\rho)}$ rad/sec					
	$\hat{\omega}_1$	$\hat{\omega}_2$	$\hat{\omega}_3$	$\hat{\omega}_4$	$\hat{\omega}_5$	$\hat{\omega}_6$
1×1	0.0779154	0.174273	0.290841			
	0.0744426	0.149078	0.244436			
2×2	0.0718554	0.163743	0.209017	0.337202	0.390486	0.396354
	0.0709672	0.154699	0.194562	0.296002	0.333969	0.344150
3×3	0.0691316	0.160807	0.193435	0.315159	0.349965	0.360910
	0.0687563	0.156454	0.186674	0.292259	0.318986	0.328831
4×4	0.0679180	0.159679	0.187012	0.302877	0.331740	0.343768
	0.0677157	0.157163	0.183210	0.289120	0.313502	0.323992
5×5	0.0672756	0.159122	0.183768	0.296001	0.322442	0.335848
	0.0671486	0.157503	0.181349	0.286947	0.310606	0.322679
6×6	0.0668951	0.158805	0.181905	0.291893	0.317093	0.331626
	0.0668080	0.157670	0.180233	0.285513	0.308840	0.322281
8×8	0.0664836	0.158471	0.179955	0.287558	0.311515	0.327497
	0.0664355	0.157830	0.179021	0.283924	0.306863	0.322123
10×10	0.0662762	0.158306	0.179009	0.285456	0.308819	0.325609
	0.0662457	0.157896	0.178414	0.283138	0.305842	0.322133
12×12	0.0661564	0.158211	0.178479	0.284287	0.307315	0.324588
	0.0661351	0.157926	0.178067	0.282672	0.305246	0.322161
Exact results (20×20)	0.0658530	0.157951	0.176908	0.279651	0.303370	0.321367

DISCUSSIONS

Extensive details of the development of a plane rectangular dynamic element have been presented that include the complete set of associated matrices. Numerical results are given in Table I for both DEM and FEM analyses, and such results are further plotted in Figures 3 and 4 to enable a clear assessment of the relative merits of the two analysis procedures.

These results clearly demonstrate that most significant improvement in root convergence is effected when dynamic elements are employed in place of the usual static finite elements. Thus, the percentage error in frequency is reduced, on the average, by a factor between 2 and 5 when dynamic elements are used for structural discretization. Also, the rate of decrease in percentage error in frequencies with increasing mesh size, as depicted by the curves in Figures 3 and 4, is considerably faster for the dynamic elements. In an effort to obtain a measure of the relative computational effort, the root convergence curves of Figure 4 may be considered. For a frequency error of 5 per cent, the FEM analysis requires 2 and 6 times the DEM solution

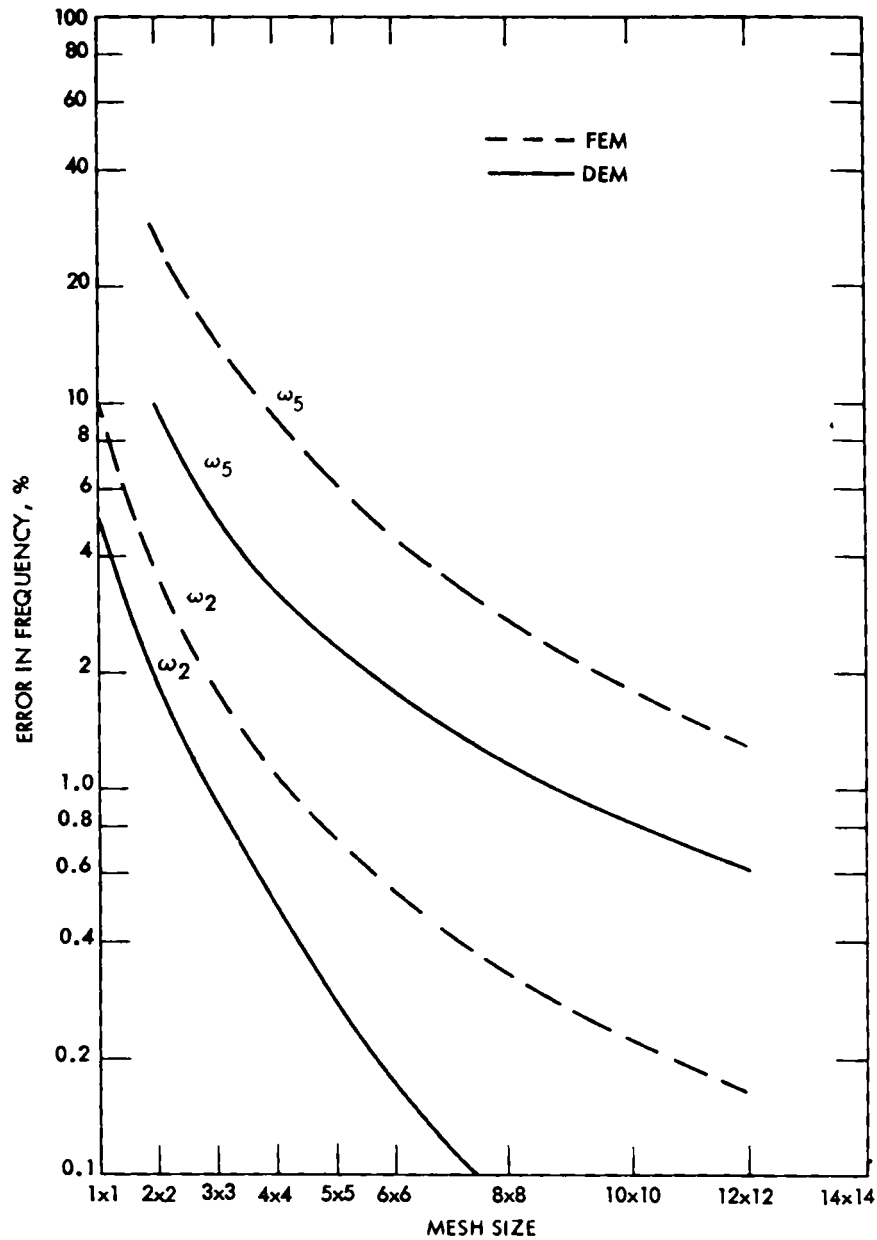


Figure 3. Convergence pattern of frequencies for a plane square element

effort for the roots ω_2 and ω_5 , respectively. Also for the same percentage error in the frequency ω_5 , the DEM analysis employing a 3×3 mesh produces about the same results as a 6×6 static finite element mesh; for a 0.5 per cent error in ω_2 the DEM and FEM analyses yield similar results with 4×4 and 6×6 meshes, respectively. Thus, the present method not only reduces the computational effort most significantly but also considerably reduces the data

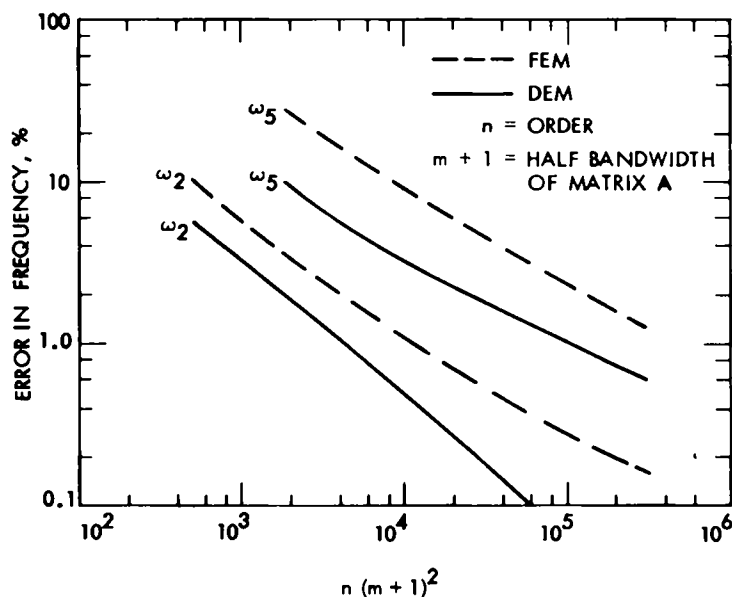


Figure 4. Plane square element: error in frequencies as a function of total numerical effort (n = order, $m + 1$ = half bandwidth of \mathbf{A})

preparation effort due to a significant reduction in mesh size for a certain desired solution accuracy.

The quadratic matrix eigenvalue procedures described herein require only a negligible increase in solution time over the usual solution methods for problems involving static finite elements. Thus, the program QMESSI (Quadratic Matrix Eigenproblem Solver based on a combined Sturm sequence and Inverse iteration technique), developed in connection with the present work and the program EASI⁷ generated earlier for the $\mathbf{A} - \omega^2 \mathbf{B}$ formulation, essentially require identical storage and solution time. The additional computational effort in QMESSI amounts to $2nm$ (NR) (NT) multiplications incurred in the triangularization of $\mathbf{A} - \omega^2 \mathbf{B} - \omega^4 \mathbf{C}$; however, since the extra effort is less than the total computational effort by a factor of m , for most practical problems this will amount to less than an order of magnitude of the total solution time. A similar observation may also be made for the simultaneous iteration procedure described elsewhere.^{3,4} Since the current solution effort is very much dependent on the matrix bandwidth, employment of a suitable bandwidth minimization routine is highly recommended prior to application of the present technique.

The key aspect in the development of the dynamic element is the appropriate choice of the vector \mathbf{a} and, more particularly, the vector \mathbf{a}_2 in equation (2). Thus, it may be observed that the usual choice of the \mathbf{a}_{0x} , \mathbf{a}_{0y} vectors given by equations (20) and (21) is such that equilibrium is not satisfied within an element, as they do not satisfy the differential equations of equilibrium, i.e., equations (14) and (17), respectively. The choice of \mathbf{a}_{2x} and \mathbf{a}_{2y} was influenced by such considerations and their current form, adopted for the present development and given by equations (22) and (23), does not also satisfy their respective equilibrium equations, namely equations (16) and (19). Also, the strains (and hence stresses) vary within an element, and since they differ from one element to another, equilibrium is usually not satisfied between elements, although equilibrium of nodal forces is satisfied. Compatibility within an element

and nodal compatibility are all easily satisfied. Interelement compatibility is also satisfied, since the deformations u_x and u_y are both linear functions of x or y along the edges.

It may be somewhat tempting to compare the performance of dynamic elements with the so-called conforming or higher order static finite elements. However, although the later elements may result in higher accuracies compared to the usual finite elements, this is not necessarily accompanied by any significant computational gain. This is due to the fact that the adoption of higher order elements is usually accompanied by an increase in the bandwidth of the associated matrices, and since the eigenproblem analysis effort is proportional to nm^2 , an increase in solution time is always resulted. In contrast, the dynamic elements effect rather substantial improvement in solution accuracy at no appreciable increase in solution time and, as such, result in a most significant economy in the entire solution effort of the free vibration problem of structures. Further research effort in the development of various other dynamic elements is expected to continue at JPL because of the obvious advantages of such a structural discretization procedure.

CONCLUSIONS

A new dynamic element for the discretization of two-dimensional structures has been presented. Also a summary is given of the associated quadratic matrix eigenproblem solution procedures that are numerically stable and that fully exploit matrix sparsity inherent in a finite element idealization. A dynamic element discretization coupled with an appropriate eigenproblem solver will result in a most significant economy in the free vibration analysis of structures when compared with other existing analysis procedures.

REFERENCES

1. J. S. Przemieniecki, *Theory of Matrix Structural Analysis*, McGraw-Hill, New York, 1968.
2. K. K. Gupta, 'Solution of quadratic matrix equations for free vibration analysis of structures', *Int. J. num. Meth. Engng*, **6**, 129-135 (1973).
3. K. K. Gupta, 'On a finite dynamic element method for free vibration analysis of structures', *Comput. Meth. Appl. Mech. Eng.*, **9**, 105-120 (1976).
4. K. K. Gupta, 'Numerical solution of quadratic matrix equations for free vibration analysis of structures', *3rd Post Conf. on Computational Aspects of Finite Element Meth.* Imperial College, London, England (1975).
5. R. Bogen, *Macsyma Reference Manual*, The Mathlab Group, M.I.T., Cambridge, Mass., 1975.
6. J. H. Wilkinson, *The Algebraic Eigenvalue Problem*, Clarendon Press, Oxford, 1965.
7. K. K. Gupta, 'Eigenproblem solution by a combined Sturm sequence and inverse iteration technique', *Int. J. num. Meth. Engng*, **7**, 17-42 (1973).

ACKNOWLEDGEMENTS

This work was sponsored by an Air Force Office of Scientific Research Grant No. AFOSR 77-3276, under the management of Lt. Col. Enrique Ramirez, whose support and encouragement is gratefully acknowledged.

APPENDIX

Subroutine for the derivation of matrices \mathbf{m}_0 , \mathbf{m}_2 , \mathbf{k}_0 , and \mathbf{k}_4 denoted by MZ, M2, KZ, and K4, respectively.

```

1      SUBROUTINE ELEMENT(MZ,M2,KZ,K4,E,MU,T,RHO,A,B,INDX)
2      C      TO COMPUTE ELEMENT STIFFNESS AND INERTIA FORCES
3      REAL MU,MZ(8,8),M2(8,8),KZ(8,8),K4(8,8),
4      1MZ(4,4),MZY(4,4),MZX(4,4),MZY(4,4)
5      C      E= YOUNG'S MODULUS, MU= POISSON'S RATIO
6      C      T= ELEMENT THICKNESS, RHO= ELEMENT MASS/UNIT AREA
7      C      A,B= ELEMENT SIDE LENGTHS IN LOCAL X,Y DIRECTIONS
8      C      INDX= 1, FOR DEM SOLUTION
9      C      = 2, FOR FEM SOLUTION
10     AL1=2.*(1.-MU)/(1.-2.*MU)
11     FF=2.*(1.+MU)*RHO/E
12     DO 6 I=1,4
13     DO 6 J=1,4
14     MZX(I,J)=0.
15     MZY(I,J)=0.
16     M2X(I,J)=0.
17     6 MZY(I,J)=0.
18     DO 7 I=1,8
19     DO 7 J=1,8
20     KZ(I,J)=0.
21     K4(I,J)=0.
22     MZ(I,J)=0.
23     7 M2(I,J)=0.
24     MZX(1,1) = 4.
25     MZX(1,2) = 2.
26     MZX(1,3) = 1.
27     MZX(1,4) = 2.
28     MZX(2,2) = 4.
29     MZX(2,3) = 2.
30     MZX(2,4) = 1.
31     MZX(3,3) = 4.
32     MZX(3,4) = 2.
33     MZX(4,4) = 4.
34     MZY(1,1) = 4.
35     MZY(1,2) = 2.
36     MZY(1,3) = 1.
37     MZY(1,4) = 2.
38     MZY(2,2) = 4.
39     MZY(2,3) = 2.
40     MZY(2,4) = 1.
41     MZY(3,3) = 4.
42     MZY(3,4) = 2.
43     MZY(4,4) = 4.
44     IF(INDX.EQ.2) GO TO 14
45     MZX(1,1) = 16*B**2+16*A**2/AL1
46     MZX(1,2) = 8*B**2+14*A**2/AL1
47     MZX(1,3) = 7*B**2+7*A**2/AL1
48     MZX(1,4) = 14*B**2+8*A**2/AL1
49     MZX(2,2) = 16*B**2+16*A**2/AL1
50     MZX(2,3) = 14*B**2+8*A**2/AL1
51     MZX(2,4) = 7*B**2+7*A**2/AL1
52     MZX(3,3) = 16*B**2+16*A**2/AL1
53     MZX(3,4) = 8*B**2+14*A**2/AL1
54     MZX(4,4) = 16*B**2+16*A**2/AL1
55     MZY(1,1) = 16*B**2/AL1+16*A**2
56     MZY(1,2) = 8*B**2/AL1+14*A**2
57     MZY(1,3) = 7*B**2/AL1+7*A**2
58     MZY(1,4) = 14*B**2/AL1+8*A**2
59     MZY(2,2) = 16*B**2/AL1+16*A**2
60     MZY(2,3) = 14*B**2/AL1+8*A**2
61     MZY(2,4) = 7*B**2/AL1+7*A**2
62     MZY(3,3) = 16*B**2/AL1+16*A**2
63     MZY(3,4) = 8*B**2/AL1+14*A**2
64     MZY(4,4) = 16*B**2/AL1+16*A**2
65     14 CONTINUE
66     KZ(1,1) = -A*MU/(6*B)+B/(3*A)+A/(6*B)

```

```

67      KZ(1,2) = MU/8+1./8.
68      KZ(1,3) = -A*MU/(12*B)-B/(3*A)+A/(12*B)
69      KZ(1,4) = 3*MU/8-1./8.
70      KZ(1,5) = A*MU/(12*B)-B/(6*A)-A/(12*B)
71      KZ(1,6) = -MU/8-1./8.
72      KZ(1,7) = A*MU/(6*B)+B/(6*A)-A/(6*B)
73      KZ(1,8) = 1./8.-3*MU/8
74      KZ(2,2) = -B*MU/(6*A)+B/(6*A)+A/(3*B)
75      KZ(2,3) = 1./8.-3*MU/8
76      KZ(2,4) = B*MU/(6*A)-B/(6*A)+A/(6*B)
77      KZ(2,5) = -MU/8-1./8.
78      KZ(2,6) = B*MU/(12*A)-B/(12*A)-A/(6*B)
79      KZ(2,7) = 3*MU/8-1./8.
80      KZ(2,8) = -B*MU/(12*A)+B/(12*A)-A/(3*B)
81      KZ(3,3) = -A*MU/(6*B)+B/(3*A)+A/(6*B)
82      KZ(3,4) = -MU/8-1./8.
83      KZ(3,5) = A*MU/(6*B)+B/(6*A)-A/(6*B)
84      KZ(3,6) = 3*MU/8-1./8.
85      KZ(3,7) = A*MU/(12*B)-B/(6*A)-A/(12*B)
86      KZ(3,8) = MU/8+1./8.
87      KZ(4,4) = -B*MU/(6*A)+B/(6*A)+A/(3*B)
88      KZ(4,5) = 1./8.-3*MU/8
89      KZ(4,6) = -B*MU/(12*A)+B/(12*A)-A/(3*B)
90      KZ(4,7) = MU/8+1./8.
91      KZ(4,8) = B*MU/(12*A)-B/(12*A)-A/(6*B)
92      KZ(5,5) = -A*MU/(6*B)+B/(3*A)+A/(6*B)
93      KZ(5,6) = MU/8+1./8.
94      KZ(5,7) = -A*MU/(12*B)-B/(3*A)+A/(12*B)
95      KZ(5,8) = 3*MU/8-1./8.
96      KZ(6,6) = -B*MU/(6*A)+B/(6*A)+A/(3*B)
97      KZ(6,7) = 1./8.-3*MU/8
98      KZ(6,8) = B*MU/(6*A)-B/(6*A)+A/(6*B)
99      KZ(7,7) = -A*MU/(6*B)+B/(3*A)+A/(6*B)
100     KZ(7,8) = -MU/8-1./8.
101     KZ(8,8) = -B*MU/(6*A)+B/(6*A)+A/(3*B)
102     IF(INDX.EQ.2) GO TO 15
103     K4(1,1) = -A*B**3*MU/1080-A**5*MU/(3780*AL1**2*B)+B**5/(1890*A)+A*
104 1    B**3/1080+A**3*B/(540*AL1**2)+A**5/(3780*AL1**2*B)
105     K4(1,2) = A**2*B**2*MU/(4608*AL1**2)+A**2*B**2*MU/4608+A**2*B**2/(
106 1    4608*AL1**2)+A**2*B**2/4608
107     K4(1,3) = -A*B**3*MU/2160-31*A**5*MU/(120960*AL1**2*B)-B**5/(1890*
108 1    A)+A*B**3/2160+7*A**3*B/(4320*AL1**2)+31*A**5/(120960*AL1**2*B)
109     K4(1,4) = -A**2*B**2*MU/(4608*AL1**2)+A**2*B**2*MU/4608+A**4*MU/(3
110 1    840*AL1)-A**2*B**2/(4608*AL1**2)+A**2*B**2/4608-A**4/(11520*AL1
111 2    )
112     K4(1,5) = -7*A*B**3*MU/17280+31*A**5*MU/(120960*AL1**2*B)-31*B**5/
113 1    (60480*A)+7*A*B**3/17280+7*A**3*B/(8640*AL1**2)-31*A**5/(120960
114 2    *AL1**2*B)
115     K4(1,6) = -B**4*MU/(11520*AL1)-A**2*B**2*MU/(4608*AL1**2)-A**2*B**
116 1    2*MU/4608-A**4*MU/(11520*AL1)-B**4/(11520*AL1)-A**2*B**2/(4608*
117 2    AL1**2)-A**2*B**2/4608-A**4/(11520*AL1)
118     K4(1,7) = -7*A*B**3*MU/8640+A**5*MU/(3780*AL1**2*B)+31*B**5/(60480
119 1    *A)+7*A*B**3/8640+A**3*B/(1080*AL1**2)-A**5/(3780*AL1**2*B)
120     K4(1,8) = -B**4*MU/(3840*AL1)+A**2*B**2*MU/(4608*AL1**2)-A**2*B**2
121 1    *MU/4608+B**4/(11520*AL1)+A**2*B**2/(4608*AL1**2)-A**2*B**2/460
122 2    8
123     K4(2,2) = -B**5*MU/(3780*A*AL1**2)-A**3*B*MU/1080+B**5/(3780*A*AL1
124 1    **2)+A*B**3/(540*AL1**2)+A**3*B/1080+A**5/(1890*B)
125     K4(2,3) = A**2*B**2*MU/(4608*AL1**2)-A**2*B**2*MU/4608-A**4*MU/(38
126 1    40*AL1)+A**2*B**2/(4608*AL1**2)-A**2*B**2/4608+A**4/(11520*AL1)
127     K4(2,4) = B**5*MU/(3780*A*AL1**2)-7*A**3*B*MU/8640-B**5/(3780*A*AL
128 1    **2)+A*B**3/(1080*AL1**2)+7*A**3*B/8640+31*A**5/(60480*B)
129     K4(2,5) = -B**4*MU/(11520*AL1)-A**2*B**2*MU/(4608*AL1**2)-A**2*B**
130 1    2*MU/4608-A**4*MU/(11520*AL1)-B**4/(11520*AL1)-A**2*B**2/(4608*
131 2    AL1**2)-A**2*B**2/4608-A**4/(11520*AL1)
132     K4(2,6) = 31*B**5*MU/(120960*A*AL1**2)-7*A**3*B*MU/17280-31*B**5/(

```

```

133 1 120900*A*AL1**2)+7*A*B**3/(8640*AL1**2)+7*A**3*B/17280-31*A**5/
134 2 (60480*B)
135 K4(2,7) = B**4*MU/(3840*AL1)-A**2*B**2*MU/(4608*AL1**2)+A**2*B**2*
136 1 MU/4608-B**4/(11520*AL1)-A**2*B**2/(4608*AL1**2)+A**2*B**2/4608
137 K4(2,8) = -31*B**5*MU/(120960*A*AL1**2)-A**3*B*MU/2160+31*B**5/(12
138 1 0960*A*AL1**2)+7*A*B**3/(4320*AL1**2)+A**3*B/2160-A**5/(1890*B)
139 K4(3,3) = -A*B**3*MU/1080-A**5*MU/(3780*AL1**2*B)+B**5/(1890*A)+A*
140 1 B**3/1080+A**3*B/(540*AL1**2)+A**5/(3780*AL1**2*B)
141 K4(3,4) = -A**2*B**2*MU/(4608*AL1**2)-A**2*B**2*MU/4608-A**2*B**2/
142 1 (4608*AL1**2)-A**2*B**2/4608
143 K4(3,5) = -7*A*B**3*MU/8640+A**5*MU/(3780*AL1**2*B)+31*B**5/(60480
144 1 *A)+7*A*B**3/8640+A**3*B/(1080*AL1**2)-A**5/(3780*AL1**2*B)
145 K4(3,6) = B**4*MU/(3840*AL1)-A**2*B**2*MU/(4608*AL1**2)+A**2*B**2*
146 1 MU/4608-B**4/(11520*AL1)-A**2*B**2/(4608*AL1**2)+A**2*B**2/4608
147 K4(3,7) = -7*A*B**3*MU/17280+31*A**5*MU/(120960*AL1**2*B)-31*B**5/
148 1 (60480*A)+7*A*B**3/17280+7*A**3*B/(8640*AL1**2)-31*A**5/(120960
149 2 *AL1**2*B)
150 K4(3,8) = B**4*MU/(11520*AL1)+A**2*B**2*MU/(4608*AL1**2)+A**2*B**2
151 1 *MU/4608+A**4*MU/(11520*AL1)+B**4/(11520*AL1)+A**2*B**2/(4608*A
152 2 L1**2)+A**2*B**2/4608+A**4/(11520*AL1)
153 K4(4,4) = -B**5*MU/(3780*A*AL1**2)-A**3*B*MU/1080+B**5/(3780*A*AL1
154 1 **2)+A*B**3/(540*AL1**2)+A**3*B/1080+A**5/(1890*B)
155 K4(4,5) = -B**4*MU/(3840*AL1)+A**2*B**2*MU/(4608*AL1**2)-A**2*B**2
156 1 *MU/4608+B**4/(11520*AL1)+A**2*B**2/(4608*AL1**2)-A**2*B**2/460
157 2 8
158 K4(4,6) = -31*B**5*MU/(120960*A*AL1**2)-A**3*B*MU/2160+31*B**5/(12
159 1 0960*A*AL1**2)+7*A*B**3/(4320*AL1**2)+A**3*B/2160-A**5/(1890*B)
160 K4(4,7) = B**4*MU/(11520*AL1)+A**2*B**2*MU/(4608*AL1**2)+A**2*B**2
161 1 *MU/4608+A**4*MU/(11520*AL1)+B**4/(11520*AL1)+A**2*B**2/(4608*A
162 2 L1**2)+A**2*B**2/4608+A**4/(11520*AL1)
163 K4(4,8) = 31*B**5*MU/(120960*A*AL1**2)-7*A**3*B*MU/17280-31*B**5/(
164 1 120960*A*AL1**2)+7*A*B**3/(8640*AL1**2)+7*A**3*B/17280-31*A**5/
165 2 (60480*B)
166 K4(5,5) = -A*B**3*MU/1080-A**5*MU/(3780*AL1**2*B)+B**5/(1890*A)+A*
167 1 B**3/1080+A**3*B/(540*AL1**2)+A**5/(3780*AL1**2*B)
168 K4(5,6) = A**2*B**2*MU/(4608*AL1**2)+A**2*B**2*MU/4608+A**2*B**2/(
169 1 4608*AL1**2)+A**2*B**2/4608
170 K4(5,7) = -A*B**3*MU/2160-31*A**5*MU/(120960*AL1**2*B)-B**5/(1890*
171 1 A)+A*B**3/2160+7*A**3*B/(4320*AL1**2)+31*A**5/(120960*AL1**2*B)
172 K4(5,8) = -A**2*B**2*MU/(4608*AL1**2)+A**2*B**2*MU/4608+A**4*MU/(3
173 1 840*AL1)-A**2*B**2/(4608*AL1**2)+A**2*B**2/4608-A**4/(11520*AL1
174 2 )
175 K4(6,6) = -B**5*MU/(3780*A*AL1**2)-A**3*B*MU/1080+B**5/(3780*A*AL1
176 1 **2)+A*B**3/(540*AL1**2)+A**3*B/1080+A**5/(1890*B)
177 K4(6,7) = A**2*B**2*MU/(4608*AL1**2)-A**2*B**2*MU/4608-A**4*MU/(38
178 1 40*AL1)+A**2*B**2/(4608*AL1**2)-A**2*B**2/4608+A**4/(11520*AL1)
179 K4(6,8) = B**5*MU/(3780*A*AL1**2)-7*A**3*B*MU/8640-B**5/(3780*A*AL
180 1 **2)+A*B**3/(1080*AL1**2)+7*A**3*B/8640+31*A**5/(60480*B)
181 K4(7,7) = -A*B**3*MU/1080-A**5*MU/(3780*AL1**2*B)+B**5/(1890*A)+A*
182 1 B**3/1080+A**3*B/(540*AL1**2)+A**5/(3780*AL1**2*B)
183 K4(7,8) = -A**2*B**2*MU/(4608*AL1**2)-A**2*B**2*MU/4608-A**2*B**2/
184 1 (4608*AL1**2)-A**2*B**2/4608
185 K4(8,8) = -B**5*MU/(3780*A*AL1**2)-A**3*B*MU/1080+B**5/(3780*A*AL1
186 1 **2)+A*B**3/(540*AL1**2)+A**3*B/1080+A**5/(1890*B)
187 15 CONTINUE
188 DO 10 I=2,4
189 I1=I-1
190 DO 10 J=1,11
191 MZX(I,J)=MZX(J,I)
192 MZY(I,J)=MZY(J,I)
193 MZX(I,J)=MZX(J,I)
194 10 MZY(I,J)=MZY(J,I)
195 DO 11 I=2,8
196 I1=I-1
197 DO 11 J=1,11
198 KZ(I,J)=KZ(J,I)

```



```

199      11 K4(I,J)=K4(J,I)
200      IX=1
201      DO 1 I=1,4
202      JX=1
203      DO 2 J=1,4
204      MZ(IX,JX)=MZ(I,J)
205      M2(IX,JX)=M2(I,J)
206      2 JX=JX+2
207      1 IX=IX+2
208      IX=2
209      DO 3 I=1,4
210      JX=2
211      DO 4 J=1,4
212      MZ(IX,JX)=MZ(I,J)
213      M2(IX,JX)=M2(I,J)
214      4 JX=JX+2
215      3 IX=IX+2
216      EM=E/(1.-MU**2)
217      FMZ=RHO*A*B/36.
218      FM2=RHO*A*B*FF/2160.
219      FKZ=EM*T
220      FK4=EM*I*FF**2
221      DO 5 I=1,8
222      DO 5 J=1,8
223      MZ(I,J)=FMZ*MZ(I,J)
224      M2(I,J)=FM2*M2(I,J)
225      KZ(I,J)=FKZ*KZ(I,J)
226      5 K4(I,J)=FK4*K4(I,J)
227      RETURN
228      END

```